

Original Article

# Telekin suppresses human hepatocellular carcinoma cells *in vitro* by inducing G<sub>2</sub>/M phase arrest via the p38 MAPK signaling pathway

Lin LI<sup>1,2,\*</sup>, Bei-bei ZHENG<sup>1,#</sup>, Li-sha MA<sup>1</sup>, Xiao SUN<sup>1</sup>, Juan-juan CHANG<sup>1</sup>, Wei-dong XIE<sup>1</sup>, Xia LI<sup>1,2,\*</sup>

<sup>1</sup>School of Ocean, Shandong University, Weihai 264209, China; <sup>2</sup>School of Pharmaceutical Sciences, Shandong University, Ji-nan 250012, China

**Aim:** Telekin, isolated from the Chinese herb *Carpesium divaricatum*, has shown anti-proliferation effects against various cancer cells, including hepatocellular carcinoma cells. In this study, we investigated the anti-proliferation mechanisms of telekin in human hepatocellular carcinoma HepG2 cells *in vitro*.

**Methods:** HepG2 cells were treated with telekin. Cell viability was evaluated using MTT assay. Flow cytometry was used to measure cell cycle profiles, ROS level and apoptosis. The protein expression levels were analyzed with Western blotting.

**Results:** Telekin (3.75–30 μmol/L) dose-dependently inhibited the viability of HepG2 cells and induced apoptosis. Furthermore, the treatment induced cell cycle arrest at G<sub>2</sub>/M phase, accompanied by significantly increased the phosphorylation of Cdc25A and Cdc2, and decreased Cyclin B1 level. Moreover, the treatment significantly stimulated ROS production, and increased the phosphorylation of p38 and MAPK-2 in the cells. Pretreatment with the antioxidant NAC (2.5, 5, and 10 mmol/L), or the p38 MAPK inhibitor SB203580 (2.5 and 5 μmol/L) dose-dependently attenuated these telekin-induced effects in the cells.

**Conclusion:** Telekin suppresses hepatocellular carcinoma cells *in vitro* by inducing G<sub>2</sub>/M phase arrest via activating the p38 MAPK pathway.

**Keywords:** Telekin; hepatocellular carcinoma; HepG2 cell; cell cycle arrest; ROS; p38 MAPK pathway; apoptosis; antioxidant; NAC; SB203580

Acta Pharmacologica Sinica (2014) 35: 1311–1322; doi: 10.1038/aps.2014.74; published online 1 Sep 2014

## Introduction

Cell division of eukaryotic cells is a highly regulated process. Cell cycle progression is regulated by a group of proteins that are expressed at cyclical levels during the cell cycle. These proteins, known as cyclin-dependent kinase complexes, are composed of cyclin-dependent kinases (CDKs) and cofactors such as cyclins<sup>[1]</sup>. Cdc2, also called maturation-promoting factor, is one of these factors<sup>[2]</sup>. Cdc2 can be activated by binding with Cyclin B1 to initiate the M phase of the cell cycle<sup>[3]</sup>. In some tumor cells, mutation of Cdc2 can eliminate the dependence of mitosis on the completion of DNA replication<sup>[4]</sup>. These findings suggest that Cdc2 is an important player in cell cycle regulation. Cdc2 can also in turn be inactivated by phosphorylation at Tyr15 and Thr14 by Wee1/Myt, leading to cell cycle arrest<sup>[1]</sup>. However, this phosphorylation status can be

regulated by Cdc25, which has been demonstrated to play an essential role in cell proliferation, apoptosis and tumorigenesis<sup>[5,6]</sup>.

To ensure the appropriate level of CDK-cyclin activation, Cdc25 phosphatase activities are tightly regulated by multiple mechanisms, including phosphorylation status and subcellular localization (binding to 14-3-3 proteins)<sup>[7]</sup>. Many researchers have demonstrated that cell cycle arrest at the G<sub>2</sub>/M-phase is usually accompanied by the phosphorylation of Cdc25. Phosphorylation of Cdc25A on S123 or S75, Cdc25B on S309 or S323, and Cdc25C on S216 creates a 14-3-3 binding site that specifically inhibits the ability of Cdc25 to interact with CDK1-cyclin B and leads to its loss of phosphatase activity or ubiquitin-mediated destruction<sup>[8]</sup>.

Mitogen-activated protein kinases (MAPKs) are serine-threonine kinases activated by various mitogens, that induce the transition of cells from a quiescent status into cell cycle division<sup>[9]</sup>. MAPKs are composed of three principal family members: extracellular signal-regulated kinase (ERK), p38 MAPK, and c-Jun amino-terminal or stress-activated protein kinase (JNK or SAPK)<sup>[10]</sup>. Previous works have suggested that p38

# These authors contributed equally to this work.

\* To whom correspondence should be addressed.

E-mail xiali@sdu.edu.cn (Xia Li)

Received 2014-04-03 Accepted 2014-07-13

MAPK participates not only in inflammatory responses but also in stress-induced signaling, cell proliferation, cell-cycle arrest, and apoptosis<sup>[11,12]</sup>. It has been reported that p38 kinase plays a critical role in the initiation of a G<sub>2</sub>/M phase delay after ultraviolet radiation or treatment with cycloheximide<sup>[13]</sup>. The activation of the p38 kinase results in the activation of MAPKAPK-2, which binds to and phosphorylates Cdc25<sup>[14,15]</sup>. *In vitro*, inhibition of p38 prevents both phosphorylation of Cdc25 and binding of 14-3-3<sup>[13]</sup>.

Hepatocellular carcinoma (HCC) is a type of cancer with increasing incidence and poor prognosis. However, no significant progress has been made in the development of effective therapeutic approaches. Screening and developing chemical compounds that can effectively inhibit HCC cell growth will have significant public health benefits. Natural products are the major source of pharmacology in general and in cancer therapy<sup>[16]</sup>. Telekin is an active eudesmane-type sesquiterpene lactone compound that is isolated from the plant *Carpesium divaricatum*, which has long been used as a Chinese folk medicine due to its antipyretic, analgesic, vermifugic, and anti-inflammatory properties<sup>[17]</sup>. Telekin has been reported to inhibit the proliferation of various cancer cells<sup>[18,19]</sup>. Our previous work demonstrated that telekin activates the mitochondria-mediated apoptotic pathway in HCC cells and exhibits the strongest cytotoxicity in HepG2 cells. Moreover, telekin can induce the accumulation of ROS, Ca<sup>2+</sup> overload, release of cytochrome *c* into the cytosol, and the activation of caspases 9 and 3<sup>[20]</sup>. In this present study, we found that telekin treatment induced an arrest in the G<sub>2</sub>/M phase in HepG2 cells. Further investigation revealed that this arrest is mediated by the p38 MAPK-mediated pathway.

## Materials and methods

### Chemical reagent

Telekin was isolated from *C. divaricatum* by Prof Weidong XIE as described previously<sup>[21]</sup>. The purified telekin (>98%) was dissolved in dimethylsulfoxide (DMSO) at 10 mmol/L as a stock solution. MTT and 4',6-diamidino-2-phenylindole (DAPI) were purchased from Sigma, USA. DCFDH-DA (2',7'-dichlorofluorescein diacetate) and NAC (*N*-acetyl-L-cysteine), SB203580 were purchased from the Beyotime Institute of Biotechnology, China. Annexin V-FITC Apoptosis Detection Kit was bought from BD Biosciences, USA. Antibodies against ERK, phospho-ERK (T202), JNK, phospho-JNK (T183), phospho-p38 (Y182), p38, phospho-MAPKAPK-2 (T222), Cdc25A, phospho-Cdc25A (S75), and Cyclin B1 were purchased from ImmunoWay. Antibodies against Cdc2 and phospho-Cdc2 (Y15) were purchased from Bioworld Technology, USA. All phospho-antibodies specifically recognize proteins phosphorylated at activation or inhibition sites. The RNeasy kit and primers for Cdc25A, Cdc2, and Cyclin B1 were brought from Sangon Biotech Co Ltd, China. All chemicals used in this study were commercial products and reagent grade.

### Cell culture

HepG2 cells were purchased from the Shanghai Institute

for Biological Sciences (SIBS), Chinese Academy of Sciences (Shanghai, China). HepG2 cells were cultured in RPMI-1640 Medium (Hyclone) containing 10% fetal bovine serum supplemented with 100 units/mL of penicillin and 100 µg/mL of streptomycin in a humidified atmosphere of 5% CO<sub>2</sub> at 37 °C.

### MTT assays

Cytotoxicities of telekin were assessed with the MTT assay. In our study, we used a p38 MAPK inhibitor SB203580, which is widely used as a specific pharmacological tool to dissect the role of p38 MAPK in various physiological processes. SB203580 is a representative pyridinylimidazole inhibitor that can highly selectively block the catalytic activity of p38 MAPK by virtue of the ability to bind to the inactive enzyme and has no inhibitory effect on JNK/SAPK and ERK<sup>[22]</sup>. The concentrations of SB203580 used here inhibited the p38 MAPK pathway specifically, which is consistent with many research studies<sup>[23,24]</sup>. HepG2 cells were seeded in 96-well plates at a density of 5×10<sup>3</sup> cells/well. After 24-h culture, cells were treated with or without SB203580 at given concentrations (2.5 and 5 µmol/L) for 1 h, and telekin was added at various concentrations (3.75, 7.5, 15, and 30 µmol/L). After 24–48 h of continuous culture, 15 µL MTT (5 g/L) was added to each well and incubated for another 4 h. IC<sub>50</sub> values were calculated from plotted results using untreated cells as 100%. Triplicate experiments were conducted in each test.

### Flow cytometry analysis of apoptosis

Annexin V-FITC Apoptosis Detection Kit was used to evaluate telekin-induced apoptosis according to the manufacturer's instructions. In summary, cells were seeded at a density of 5×10<sup>4</sup>/mL into 6-well plates. After 24-h culture, cells were pretreated with or without SB203580 (2.5 µmol/L) and then treated with various concentrations of telekin (5, 10, and 15 µmol/L) for 24 h. At the indicated timepoint, the cells were washed twice with ice-cold PBS and suspended in 400 µL of Annexin V-FITC binding buffer. The cells were then incubated with 5 µL Annexin V-FITC and 5 µL Propidium Iodide (PI) for 20 min at room temperature in the dark. The apoptotic ratio was analyzed by flow cytometry (Becton Dickinson, USA) and Win MDI 2.9 analysis software. Annexin V-positive and Annexin V/PI-positive cells were considered apoptotic.

### DAPI staining

To observe the morphological changes of the nuclei, HepG2 cells were seeded on 12-mm round glass cover slips in 24-well plates at a density of 5×10<sup>4</sup>/mL. After 24-h incubation, the cells were treated with telekin (5, 10, and 15 µmol/L) for 24 h. After the cells were washed with cold PBS, cold-methyl alcohol/acetone (1:1 *v/v*) was used to fix cells. The cells were subsequently washed with PBS and stained with DAPI (4 µg/mL) for 10 min at room temperature. Cover slips containing the cells were then washed by PBS-TX (10 mL PBS+10 µL 10% Tritonx-100) three times and mounted using mounting medium (PBS: Glycerol=1:1 *v/v*) and analyzed by fluorescence microscopy (Leica DM IRB).

### Measurement of ROS generation

Oxidative stimuli found in the cytoplasm may be transmitted through cellular signal transduction pathways to the nucleus to direct cell division and survival. We evaluated the changes in intracellular ROS levels using DCFH-DA. DCFH-DA can change into fluorescent dichlorofluorescein (DCF) when intracellular DCFH reacts with ROS. HepG2 cells were grown in 6-well plates, pretreated with or without NAC (2.5, 5, and 10 mmol/L), and then treated with 15  $\mu\text{mol/L}$  telekin for 6–24 h. After incubation, the culture medium was removed, and the cells were washed three times with PBS. The cells were incubated with DCFH-DA (3  $\mu\text{mol/L}$ ) at 37°C for 20 min. Cellular fluorescence was measured by flow cytometry with a FACS-SCAN apparatus. Increased values relative to the control were considered to represent an increase in the intracellular ROS level.

### RNA extraction and relative quantification by real-time PCR

HepG2 cells were grown in 6-well plates, pretreated with or without SB203580 (2.5 and 5  $\mu\text{mol/L}$ ), and treated with telekin (5, 10, and 15  $\mu\text{mol/L}$ ) for 12 h. An RNeasy kit was used to extract total RNA according to the manufacturer's instructions. The purity of RNA was checked by the  $OD_{260/280}$  of the RNA samples ( $>1.8$ ). Then, DNA was synthesized through reverse transcription using M-MLV Reverse Transcriptase and Oligo (dT) primers. Real-time PCR assay was used to detect the expression of the Cdc25A, Cdc2, and Cyclin B1 genes. PCR amplification was performed in an 8-tube strip format (Axygen, Union City, CA) in triplicate. Each reaction contained 1 $\times$ SYBR Green PCR Master mix, 1  $\mu\text{L}$  forward primer and reverse primer and 1  $\mu\text{L}$  template cDNA in a final volume of 20  $\mu\text{L}$  using a Mastercycler eprealplex apparatus (Eppendorf, Germany). Primers were designed for the Cdc25 A gene (sense: 5'-ACAGCTCCTCTCGTCATGAGAAC-3' and antisense: 5'-GGTCTCTTCAACACTGACCGAGT-3'), Cdc2 gene (sense: 5'-TACATTTCCCAAATGGAAACCAG-3' and antisense: 5'-AAT TCGTTTGGCTGGATCATAGA-3'), and Cyclin B1 gene (sense: 5'-AGGAAGAGCAAGCAGTCAGAC-3', and antisense: 5'-GCAGCATCTTCTTGGGCACAC-3'). The GAPDH gene (sense: 5'-CCATGGAGAAGGCTGGGG-3' and antisense: 5'-CAAAGTTGTCATGGATGACC-3') was used as a control of the RNA amount. Amplification was performed for 45 cycles of sequential denaturation (95°C, 2 min), annealing (60°C, 15 s), and extension (72°C, 20 s). Data acquisition and the analysis of real-time PCR assays were performed using the Mastercycler eprealplex. Each fluorescent reporter signal was measured against the internal reference dye signal to normalize for non-PCR-related fluorescence fluctuations between wells. All samples were measured in triplicate independent experiments.

### Cell cycle distribution

To evaluate the role of ROS, NAC (*N*-acetyl-*L*-cysteine) was used in our experiments. NAC is a widely used thiol-containing antioxidant that is a precursor of reduced glutathione (GSH). GSH scavenges ROS in cells by interacting with OH $\cdot$

and H $_2$ O $_2$ , thus affecting ROS-mediated signaling pathways<sup>[25]</sup>. HepG2 cells were seeded into 6-well plates and pretreated with or without SB203580 (2.5 and 5  $\mu\text{mol/L}$ ) or NAC (2.5, 5, and 10 mmol/L) for 1 h, then treated with various concentrations of telekin at 37°C for 24 h. The cells were washed twice with ice-cold PBS and fixed with 70% alcohol. After incubating for 10 h at 4°C, cells were treated with RNase (150  $\mu\text{g/mL}$ ) for 30 min at 37°C and were subsequently stained with propidium iodide (50  $\mu\text{g/mL}$ ) for 1 h at 4°C. The cell cycle distribution was examined by flow cytometry, and the data were analyzed using the Modfit program (Becton Dickinson, USA).

### Western blotting analysis

Cells were treated with or without SB203580 (2.5 and 5  $\mu\text{mol/L}$ ) and NAC (2.5, 5, and 10 mmol/L) and were incubated with indicated concentrations of telekin for 24 h. Whole cell lysates were denatured by boiling with 1 $\times$ Laemmli buffer, separated with 10% SDS-polyacrylamide gel electrophoresis and were transferred to a nitrocellulose membrane. The membrane was washed with distilled water and then blocked with 8% non-fat milk in TBST buffer (10 mmol/L Tris-HCl, 150 mmol/L NaCl, and 0.05% *v/v* Tween-20, pH 7.8) for at least 1 h at room temperature. After a brief wash in TBST buffer, the membrane was probed with monoclonal antibodies specific against phospho-p38, p38, ERK, phospho-ERK, JNK, phospho-JNK, phospho-MAPKAPK-2, Cdc25A, phospho-Cdc25A, Cyclin B1, Cdc2, phospho-Cdc2, and GAPDH (diluted 1:800) overnight at 4°C. After washing with TBST buffer, the membranes were incubated with secondary HRP-conjugated goat anti-mouse IgG or anti-rabbit IgG. Proteins on the membranes were visualized using the enhanced chemiluminescence detection system (ECL<sup>®</sup>, Amersham Biosciences). Protein expression density values were quantified by densitometry using the Image J and Java software.

### Statistical analysis

Statistical analysis was conducted by using an analysis of variance (ANOVA) followed by Turkey's *t*-test. *P*-values less than 0.05 were considered statistically significant. All experiments were repeated at minimum in triplicate.

## Results

### Telekin arrests cells cycle at the G $_2$ /M phase

Telekin, an active eudesmane-type sesquiterpene lactone compound, was isolated from the plant *C. divaricatum*. Its structure is presented in Figure 1. To investigate the effect of telekin on cell growth, we examined the cell cycle distribution of HepG2

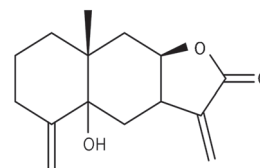
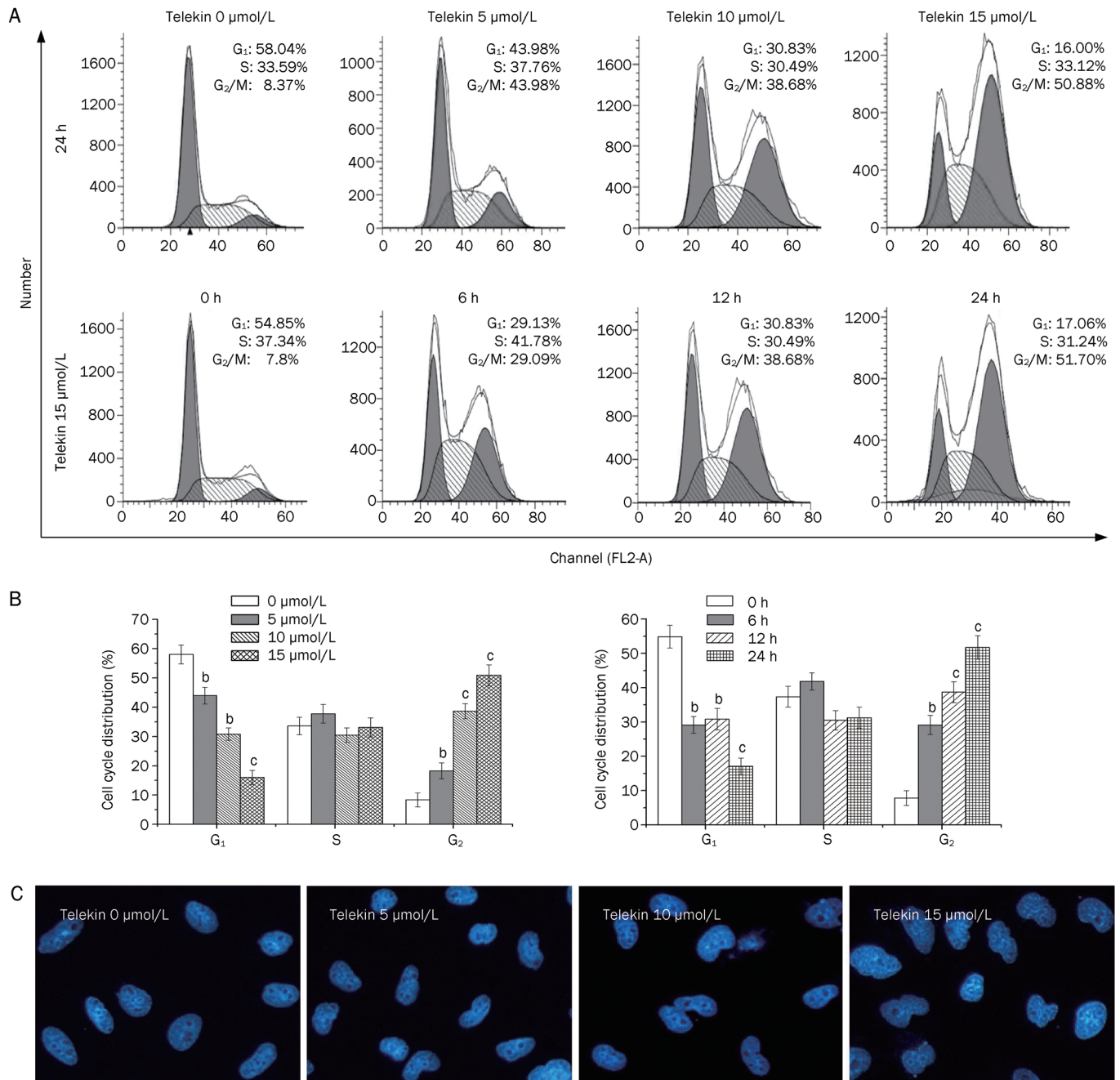


Figure 1. Chemical structure of telekin.

cells after exposure to telekin at 5, 10, and 15  $\mu\text{mol/L}$  for 24 h. As shown in Figure 2A, treatment with telekin increased the proportion of HepG2 cells in the  $G_2/M$  phase and decreased the proportion in the  $G_1$ -phase. This effect was dose- and time-dependent. The significant increase in the  $G_2/M$  population was observed at the 24 h timepoint after telekin treatment at a concentration of 15  $\mu\text{mol/L}$  (50.88%).

DAPI (4',6-diamidino-2-phenylindole dihydrochloride) can

combine specifically with DNA, and DNA-DAPI complexes emit bluish white fluorescence with maximal intensity at 450 nm when excited by ultraviolet light<sup>[26]</sup>. This fluorochrome has been used as a qualitative probe for DNA molecules because of its high sensitivity. In many previous studies, DAPI staining was used to observe changes in nucleus morphology<sup>[27]</sup>. Here, DAPI staining was employed to confirm that the effect of telekin on DNA replication and changes in nuclear morphology.



**Figure 2.** Telekin-induced cell-cycle arrest at the  $G_2/M$  phase. HepG2 cells were treated for 24 h with various concentrations of telekin (0–15  $\mu\text{mol/L}$ ) or with 15  $\mu\text{mol/L}$  telekin for various time (0–24 h). (A) The cell cycle distribution was measured using flow cytometry. (B) The histograms indicate the cell cycle distribution in HepG2 cells treated with telekin. <sup>b</sup> $P < 0.05$ , <sup>c</sup> $P < 0.01$  vs 0  $\mu\text{mol/L}$  telekin group. (C) HepG2 cells were stained with DAPI to determine the morphology of nucleus. Treatment with telekin resulted in nuclei unable to segregate after DNA replication. DAPI: 4',6-diamidino-2-phenylindole.

In our study, HepG2 cells were treated with telekin (5, 10, and 15  $\mu\text{mol/L}$ ) and stained with DAPI to determine the morphology of the nuclei. Telekin caused an increase in the number of large nuclei, which contain increased DNA levels (Figure 2C), suggesting that HepG2 cells had completed DNA replication. These data demonstrate that these cells passed the S-phase and did not enter the M-phase.

### Telekin induced regulators of G<sub>2</sub>/M phase transition

We analyzed the protein levels of the regulators of the G<sub>2</sub>/M phase, including Cdc25A, phospho-Cdc25A, Cdc2, phospho-Cdc2, and Cyclin B1 using Western blotting following telekin treatment. As shown in Figure 3A, telekin significantly increased the level of phospho-Cdc25A and phospho-Cdc2, but decreased that of Cdc25A, Cdc2, and Cyclin B1. This effect was dose-dependent.

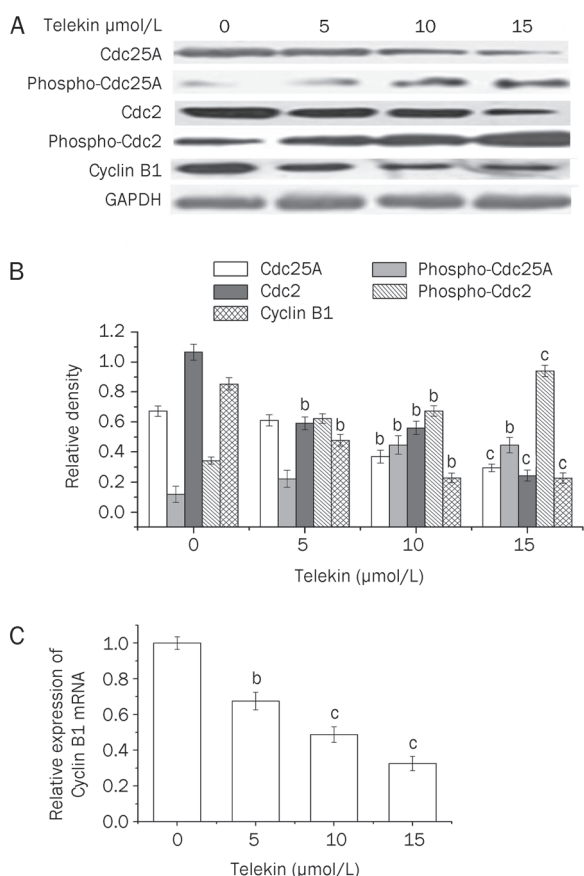


**Figure 3.** Telekin induced regulators of G<sub>2</sub>/M phase initiation. (A) Telekin induced expression changes in some proteins involved in the G<sub>2</sub>/M phase. Cells treated with 0, 5, 10, and 15  $\mu\text{mol/L}$  of telekin for 24 h were subjected to Western blotting assay. Telekin decreased the expression of Cdc25A, Cdc2, and Cyclin B1 and increased the expression of phospho-Cdc25A and phospho-Cdc2 in HepG2 cells. (B) The corresponding histograms quantified by densitometry are presented under the blots. (C) We performed qRT-PCR analysis to detect the mRNA level of Cyclin B1. HepG2 cells treated with 0, 5, 10, and 15  $\mu\text{mol/L}$  of telekin for 12 h were subjected to qRT-PCR analysis. The results indicate that telekin decreased the level of Cyclin B1 mRNA. <sup>b</sup> $P < 0.05$ , <sup>c</sup> $P < 0.01$  vs 0  $\mu\text{mol/L}$  telekin group.

The decreased Cyclin B1 level was somewhat surprising. We performed qRT-PCR analysis to clarify this point. Telekin treatment caused a decrease in the level of Cyclin B1 mRNA (Figure 3C). Cdc2 was activated by binding Cyclin B1 and initiating the M phase of the cell cycle. Cyclin B1 is likely the primary regulator of mammalian mitosis<sup>[28]</sup>. Some chemical compounds have been reported to induce G<sub>2</sub>/M phase arrest by decreasing the intracellular levels of Cyclin B1<sup>[29, 30]</sup>, which is consistent with our work. In this study, telekin induced a decrease in Cyclin B1 mRNA and protein levels.

### Telekin induced protein activation and ROS generation

We employed the Western blotting technique to evaluate changes in the levels of the major members of the MAPKs signaling pathway, such as ERK, phospho-ERK, JNK, phospho-JNK, p38, phospho-p38, and phospho-MAPKAPK-2 after the cells were treated with telekin. As shown in Figure 4A, treatment with telekin significantly increased the level of phospho-p38 and phospho-MAPKAPK-2. Additionally, this effect was dose-dependent. However, the level of p38, ERK, phospho-ERK, JNK, and phospho-JNK did not change significantly. These results suggested that p38 MAPK may play a role in the effect of telekin on cell cycle regulation.

Many studies have demonstrated that ROS plays a central role in the induction of apoptosis via a variety of mechanisms. ROS generation can activate the MAPK family member cascade, which was involved in cell cycle regulation. To determine whether telekin can induce the generation of ROS, we measured the DCF-derived fluorescence by flow cytometric assay. As shown in Figure 4B, telekin induced ROS accumulation (15  $\mu\text{mol/L}$  for 6–24 h) in HepG2 cells. This effect was time-dependent. Therefore, telekin likely induced cell cycle G<sub>2</sub>/M phase arrest by inducing ROS accumulation followed by the activation of the MAPK network.

### Elimination of ROS blocked telekin-mediated cell cycle arrest

To confirm the involvement of ROS in telekin-induced p38 MAPK-mediated G<sub>2</sub>/M phase cell cycle arrest, HepG2 cells were pretreated with NAC, which is a widely used thiol-containing antioxidant that is a precursor of reduced glutathione (GSH)<sup>[31]</sup>, before exposure to telekin. Figure 5 demonstrates that pretreatment with NAC (2.5–10 mmol/L) resulted in the inhibition of both the generation of ROS and the ability of telekin to induce G<sub>2</sub>/M phase cell cycle arrest. When HepG2 cells were pretreated with NAC (2.5, 5, and 10 mmol/L), the level of ROS and the percentage of cells in the G<sub>2</sub>/M phase decreased significantly compared with the cells treated with telekin (15  $\mu\text{mol/L}$ ) only. Furthermore, the changes in the levels of phospho-p38, phospho-MAPKAPK-2, Cdc25A, and Cdc2 were reduced when compared with cells treated with telekin only (Figure 6). These data confirmed that ROS plays an important role in telekin-induced cell cycle arrest.

### Inhibition of p38 MAPK blocked telekin-mediated cell cycle arrest

To further confirm the involvement of p38 MAPK in telekin-

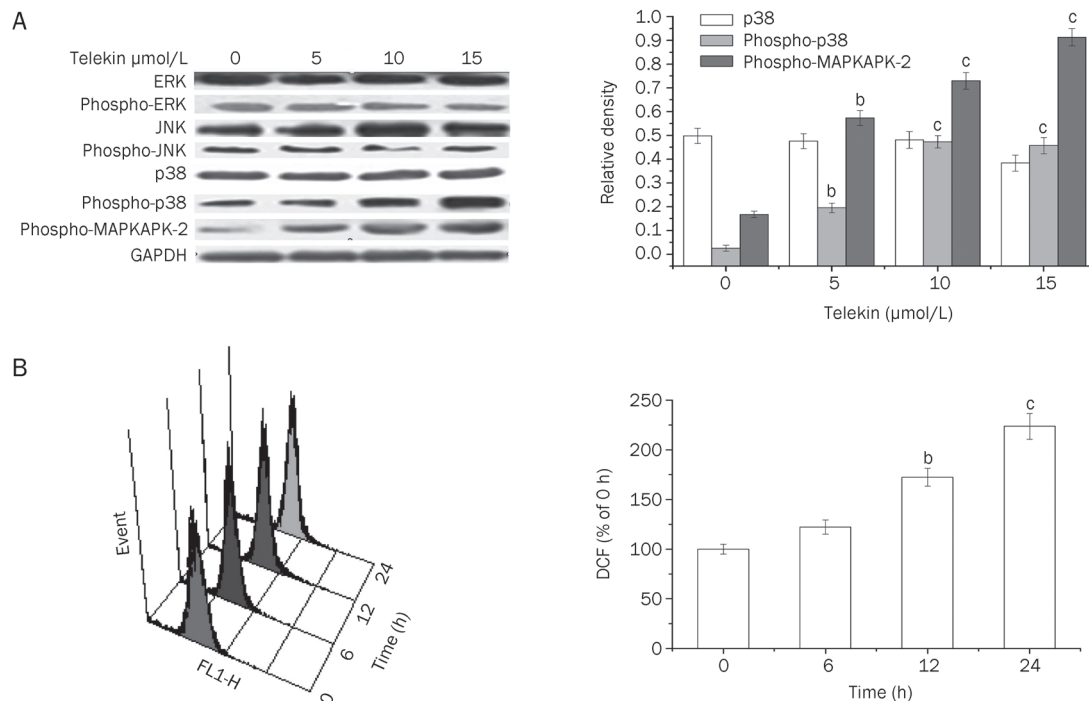


**Figure 4.** Telekin induced protein activation and ROS generation. (A) Telekin induced the activation of p38 MAPK. Cells treated with 0, 5, 10, and 15  $\mu\text{mol/L}$  of telekin for 24 h were subjected to Western blotting assay. Telekin induced an increase in phospho-p38 and phospho-MAPKAPK-2 level in a dose-dependent manner. However, the levels of ERK, phospho-ERK, JNK, and phospho-JNK did not change notably. The corresponding histograms quantified by densitometry are presented on the right. <sup>b</sup> $P < 0.05$ , <sup>c</sup> $P < 0.01$  vs 0  $\mu\text{mol/L}$  telekin group. (B) The representative ROS pattern and the corresponding histograms of HepG2 cells were examined by flow cytometric analysis. The fluorescence intensity of cells without telekin treatment was set as 100% (0 h telekin group). <sup>b</sup> $P < 0.05$ , <sup>c</sup> $P < 0.01$  vs 0 h telekin group.

induced  $G_2/M$  phase cell cycle arrest, HepG2 cells were pretreated with the p38 MAPK signaling pathway inhibitor, SB203580, before being exposed to telekin<sup>[32]</sup>. The results revealed that pretreatment with SB203580 (2.5  $\mu\text{mol/L}$ ) resulted in the inhibition of the ability of telekin to induce  $G_2/M$  phase cell cycle arrest and decreased the percentage of cells in  $G_2/M$  phase (Figure 7). These data confirmed that p38 MAPK is involved in telekin-induced cell cycle arrest.

#### Inhibition of p38 reversed the expression of $G_2/M$ phase regulators

To further test the role of p38 MAPK in telekin-induced  $G_2/M$  phase cell cycle arrest, we used western blotting to evaluate the expression of  $G_2/M$  phase regulators in cells pretreated with SB203580. As shown in Figure 8A, when cells were pretreated with 2.5 or 5  $\mu\text{mol/L}$  SB203580, the expression of phospho-p38 and phospho-MAPKAPK-2 decreased, and Cdc25A and Cdc2 increased when compared with the cells treated with telekin only. These results further confirmed the involvement of p38 MAPK in telekin-induced  $G_2/M$  phase cell cycle arrest.

Using qRT-PCR analysis, we found that the mRNA levels of Cdc25A and Cdc2 were markedly downregulated after 12-h telekin (5 or 15  $\mu\text{mol/L}$ ) treatment (Figure 8C). Furthermore, SB203580 could reverse the changes in mRNA levels.

Furthermore, we also tested the effect of NAC and SB203580

on the expression p38, phospho-p38, phospho-MAPKAPK-2, Cdc25A, and Cdc2 by Western blotting. The inhibitors (NAC and SB203580) exhibited little influence on the expression level of the regulators (Figure 9A).

#### Inhibition of p38 MAPK decreased the cytotoxicity of telekin

As described above, we observed that the effect of telekin-induced cell cycle arrest was mediated by the p38 MAPK pathway. Next, we determined whether p38 MAPK mediated the cytotoxic effect of telekin. To achieve this goal, we performed MTT assays to determine and assess the cytotoxic effect of telekin on HepG2 cells. As shown in Figure 9B, after treating the cells with 15  $\mu\text{mol/L}$  telekin, the percentage of viable cells (48 h) increased from 31.7% to 48.4% and 61.8% when the cells were pretreated with 2.5 and 5  $\mu\text{mol/L}$  SB203580, respectively. Furthermore, we also detected the toxicity of SB203580 alone; the  $\text{IC}_{50}$  of SB203580 in HepG2 cells was 100  $\mu\text{mol/L}$ . Moreover, SB203580 at 2.5 or 5  $\mu\text{mol/L}$  concentrations did not exhibit any toxicity toward HepG2 cells.

#### Inhibition of p38 MAPK decreased the apoptotic effect of telekin

To determine the possible inhibition effect of SB203580 on telekin-induced apoptosis, we quantitatively analyzed the apoptosis induced by telekin through flow cytometry using the Annexin V-FITC and propidium iodide double-staining method. When the cells were pretreated with 2.5  $\mu\text{mol/L}$

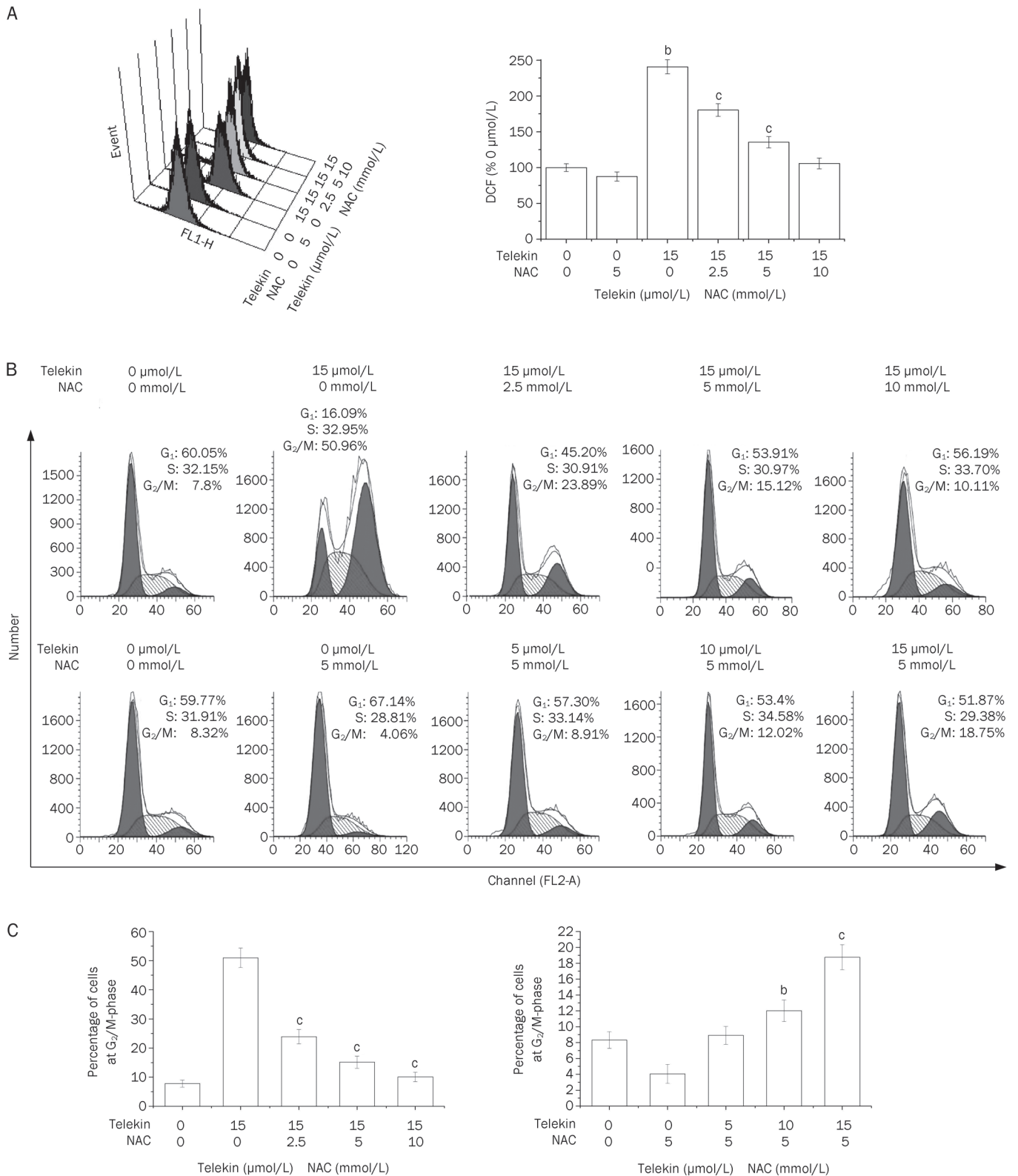


**Figure 5.** Eliminating ROS blocked telekin-mediated cell cycle arrest. HepG2 cells were pretreated with 0, 2.5, 5, or 10 mmol/L NAC and treated with 15 μmol/L telekin or were pretreated with 5 mmol/L NAC for 1 h and then treated with 0, 5, 10, or 15 μmol/L telekin for 24 h. (A) NAC treatment decreased the ROS generation significantly. <sup>b</sup>*P*<0.05, <sup>c</sup>*P*<0.01 vs 0 μmol/L telekin+5 mmol/L NAC group. (B) NAC treatment decreased the percentage of cells in the G<sub>2</sub>/M phase. The percentage of cells in the G<sub>2</sub>/M phase decreased from 50.88% to 18.7% (5 mmol/L NAC). (C) The corresponding histograms are presented below. <sup>b</sup>*P*<0.05, <sup>c</sup>*P*<0.01 vs 15 μmol/L telekin+0 mmol/L NAC group, or 0 μmol/L telekin+5 mmol/L NAC group.

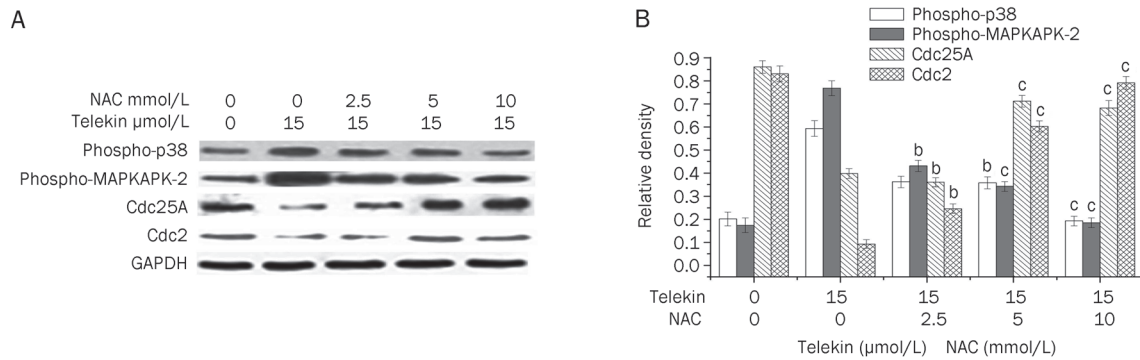


**Figure 6.** Inhibition of ROS reversed the changes of some major proteins. HepG2 cells were pretreated with NAC (0, 2.5, 5, and 10 mmol/L) and then treated with 15  $\mu\text{mol/L}$  telekin for 24 h. Protein expression was determined by Western blotting. (A) As shown, pretreatment of cells with NAC decreased the expression of phosphor-p38 and phospho-MAPKAPK-2 and increased the expression of Cdc25A and Cdc2 compared with the cells treated with telekin only. (B) The corresponding histograms quantified by densitometry are expressed on the right side. <sup>b</sup> $P < 0.05$ , <sup>c</sup> $P < 0.01$  vs 15  $\mu\text{mol/L}$  telekin+0 mmol/L NAC group.

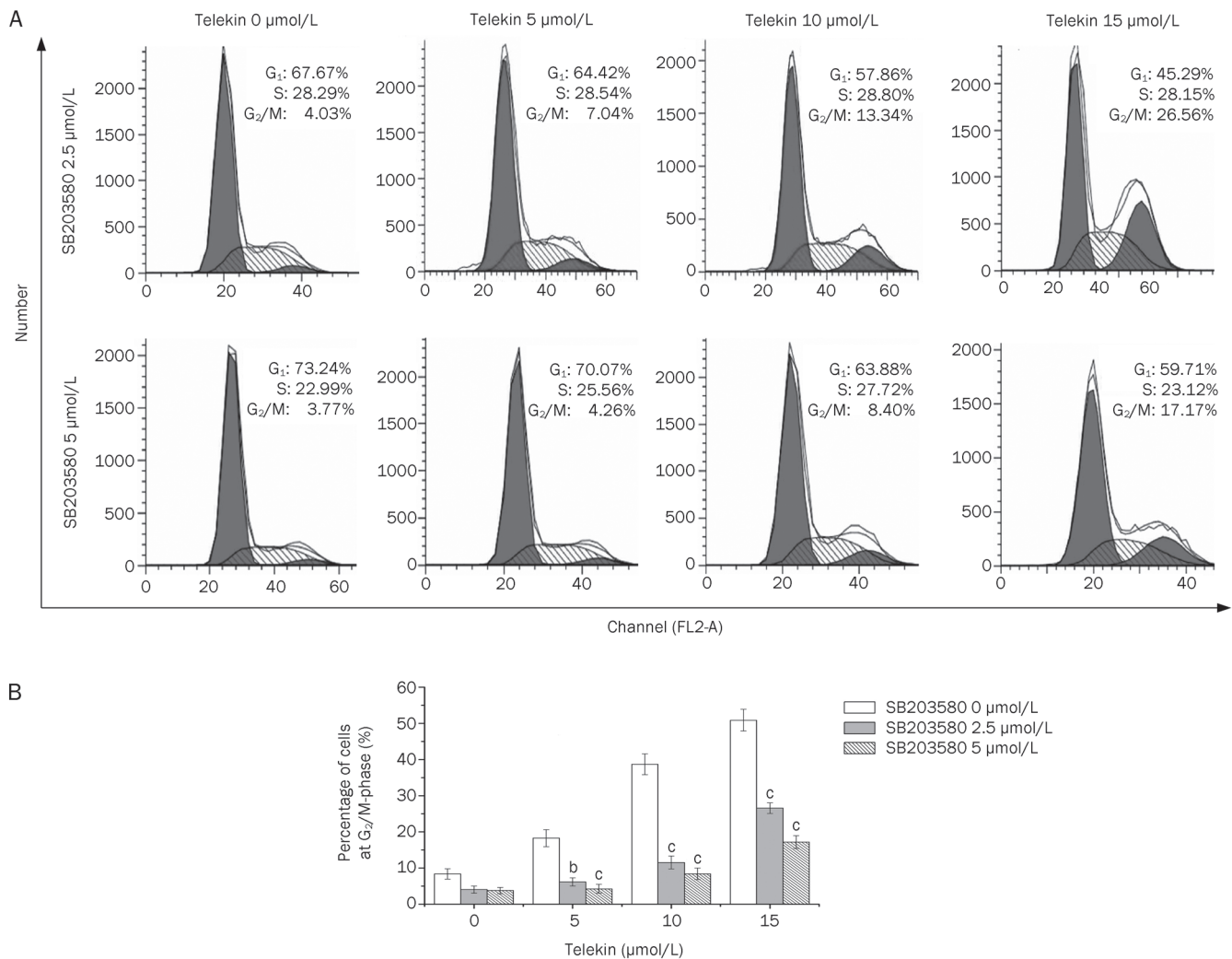


**Figure 7.** The p38 inhibitor SB203580 attenuated cell cycle arrest. HepG2 cells were pretreated with the indicated concentrations of SB203580 for 1 h and then treated with various concentrations of telekin (0, 5, 10, and 15  $\mu\text{mol/L}$ ) for 24 h. (A) SB203580 treatment decreased the percentage of cells in the G<sub>2</sub>/M phase from 50.88% to 26.56% (2.5  $\mu\text{mol/L}$  SB203580) and 17.17% (5  $\mu\text{mol/L}$  SB203580) after 24-h treatment with 15  $\mu\text{mol/L}$  telekin. Inhibiting the activity of p38 attenuated the effect of telekin on cell cycle regulation. (B) The corresponding histograms were obtained from triplicate experiments and are presented at the bottom of the figure. <sup>b</sup> $P < 0.05$ , <sup>c</sup> $P < 0.01$  vs 0  $\mu\text{mol/L}$  SB203580 group.



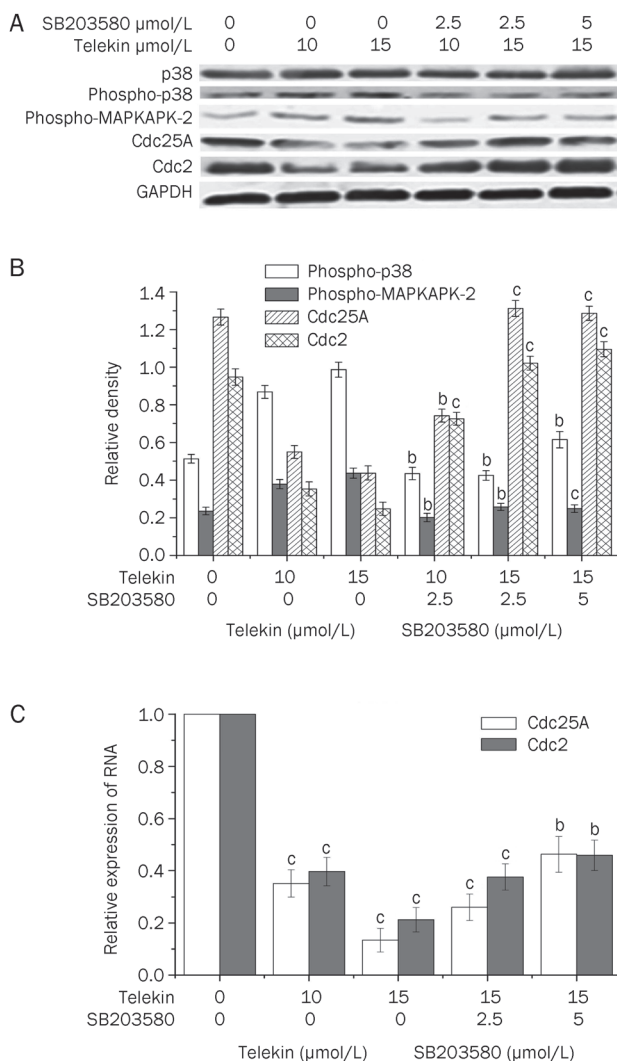


**Figure 8.** Inhibition of p38 reversed the changes of some major proteins. (A) As shown, pretreatment of cells with SB203580 decreased the expression of phospho-p38 and increased the activity of Cdc25A and Cdc2 compared with that of the cells treated with telekin only. (B) The corresponding histograms quantified by densitometry are expressed below part A. <sup>b</sup> $P < 0.05$ , <sup>c</sup> $P < 0.01$  vs 0 μmol/L SB203580 group. (C) Relative expression of Cdc25A and Cdc2 mRNA in the HepG2 cells. The relative levels of Cdc25A and Cdc2 mRNA were determined by relative quantification by real-time PCR. RNA levels (normalized to GAPDH mRNA level) are represented as fold decrease relative to the level of the control strain. <sup>b</sup> $P < 0.05$ , <sup>c</sup> $P < 0.01$  vs 0 μmol/L telekin group.

SB203580, the fraction of apoptotic cells (early apoptotic and late apoptotic) decreased from 49.45% to 31.8% when treated with 15 μmol/L telekin for 24 h. Annexin V-positive cells were considered early apoptotic cells, and Annexin V/PI-positive cells were considered late apoptotic/necrotic cells. Representative cell apoptosis patterns observed in our flow cytometric analysis are presented in Figure 10A. These results demonstrate that p38 MAPK mediated the cytotoxic and apoptosis-inducing effect of telekin. Therefore, we can conclude that the inhibitory effect of telekin on cancer proliferation is at

least partially mediated through the p38 MAPK pathway.

## Discussion

In recent years, compounds derived from plants are becoming increasingly important sources for the development of anticancer drugs. Chinese herbs are composed of active components that are able to regulate cell activities. Telekin is one of these compounds, and isolation from *C. divaricatum* by our laboratory was described in a previous report<sup>[21]</sup>.

It has been reported that an increase in oxidative stress is associated with an apoptotic response induced by several anticancer agents. ROS can cause cell apoptosis via a variety of mechanisms. One of these mechanisms is the activation of MAPKs<sup>[33]</sup>. MAPKs are activated by the dual phosphorylation of threonine and tyrosine residues by upstream kinases. For example, p38 MAPK is activated by dual phosphorylation on Thr180 and Tyr182 in a Thr-Gly-Tyr activation loop<sup>[34, 35]</sup>. Previous work has demonstrated that an accumulation of ROS can induce p38 MAPK phosphorylation. This process can be inhibited by rotenone, thenoyltrifluoroacetone, myxothiazol, and inhibitors of mitochondrial complexes I, II, and III. These data suggest that ROS leads to p38 phosphorylation through a mechanism that requires electron flux in the proximal region of the mitochondrial electron transport chain<sup>[36]</sup>. Moreover, some reports demonstrated that NAC is able to attenuate the activity of p38 MAPK against oxidative stress-induced cell death. In this mechanism, pretreatment with NAC significantly inhibited the levels of phosphorylated p38 MAPK, but the levels of nonphosphorylated p38 MAPK were unaffected<sup>[37]</sup>. Our studies demonstrates that telekin-induced ROS generation occurs in a time- and dose-dependent manner, and ROS affects the activation of p38 MAPK and cell cycle arrest. It is worth exploring the involvement of p38 MAPK in the effect of telekin.

p38 MAPK is involved in the stress response that is conserved in eukaryotic cells from yeast to mammals. Some studies indicate that the p38 MAPK cascade is involved in the apoptotic pathway of human hepatoma cell lines. The activity levels of p38 MAPK and MKK6 (which is upstream of p38 MAPK) in human HCC cells are significantly lower compared with that of non-tumorous liver tissue, suggesting that the attenuation of the p38 MAPK activities may account for the resistance to apoptosis. This resistance can in turn cause unrestricted cell growth<sup>[38]</sup>. p38 kinase has been shown to be an essential factor for sustained G<sub>2</sub>/M arrest induced by irradiation, oxidant stresses, decitabine, vanadate, and chemicals<sup>[39]</sup>. The activation of the p38 kinase results in the activation of MAPKAPK-2, which phosphorylates Cdc25, thereby reducing the activity of Cdc25 and leading to a subsequent increase in Cdc2 phosphorylation<sup>[40, 41]</sup>.

In the present study, we found that activation of p38 was involved in the accumulation of inactive phospho-Cdc2, which may be due to the decrease in Cdc25 activation by phosphorylation, causing the subsequent G<sub>2</sub>/M arrest. Cdc25 is reported to be highly regulated by multiple post-translational modifications within its N-terminal regulatory domain and site-specific

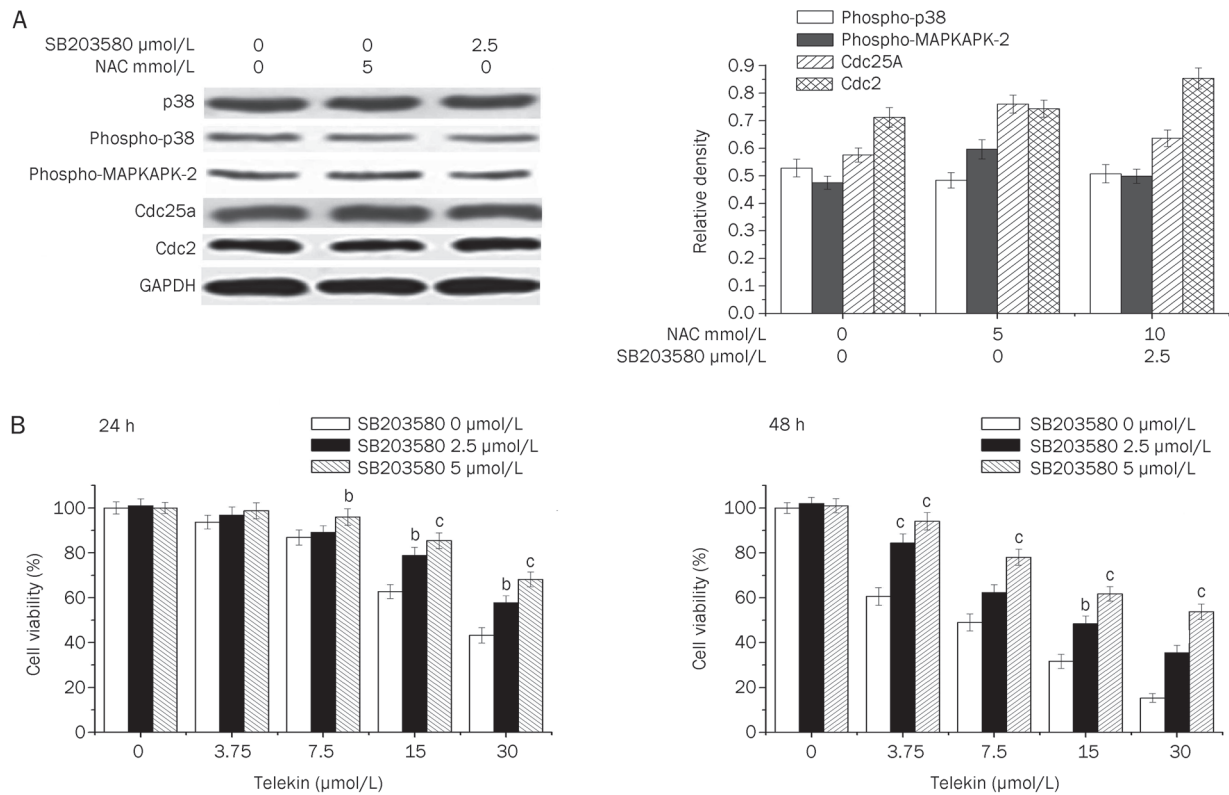


**Figure 9.** Inhibition of p38 activity decreased the cytotoxicity effect of telekin. (A) Effect of NAC and SB203580 on protein expression. As shown, treatment of HepG2 cells with NAC (5 mmol/L) and SB203580 (5  $\mu\text{mol/L}$ ) for 24 h did not change the expression levels of p38, phospho-p38, phospho-MAPKAPK-2, Cdc25A, or Cdc2. The corresponding histograms quantified by densitometry are expressed on the right side. (B) HepG2 cells were treated with various concentrations of telekin and 0-5  $\mu\text{mol/L}$  SB203580, respectively for 24 h (A) and 48 h (B). Data were obtained from triplicate experiments. <sup>b</sup> $P < 0.05$ , <sup>c</sup> $P < 0.01$  vs 0  $\mu\text{mol/L}$  SB203580 group.

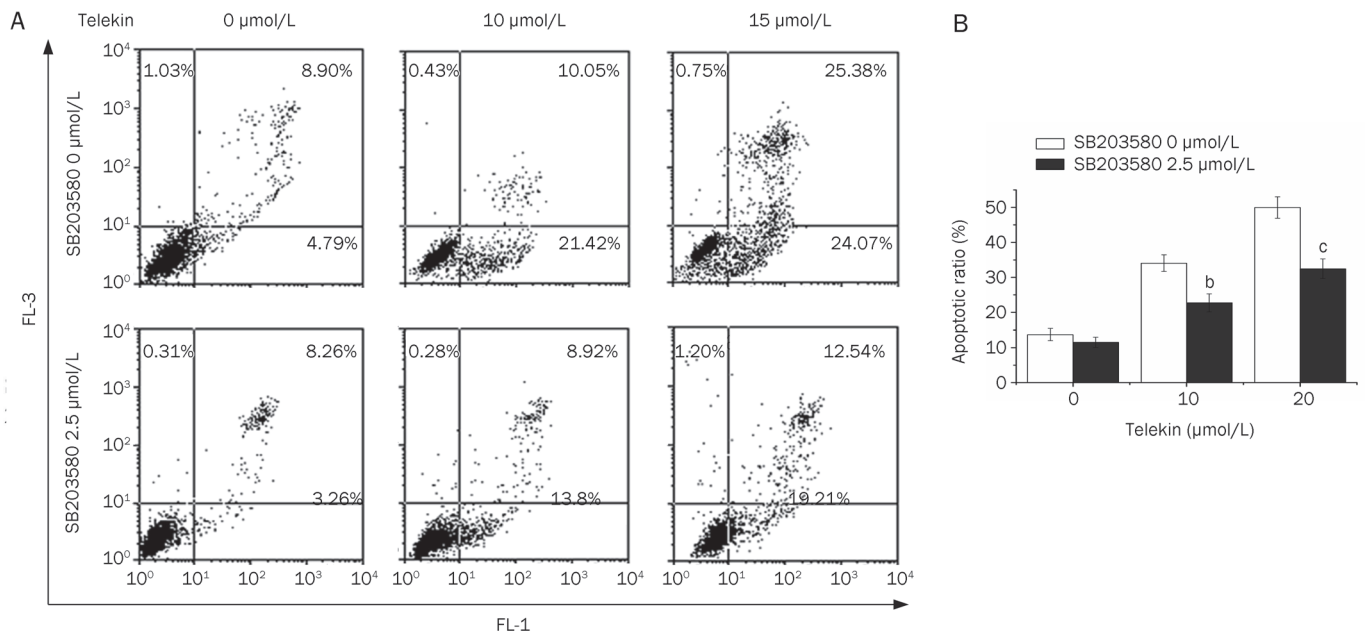


**Figure 10.** Inhibition of p38 decreased telekin-induced apoptosis. (A) Representative apoptotic profile of HepG2 cells treated with or without telekin and SB203580 by flow cytometric analysis. (B) Quantification of telekin induced-apoptosis was performed using flow cytometric analysis. Histograms were obtained from triplicate experiments. <sup>b</sup> $P < 0.05$ , <sup>c</sup> $P < 0.01$  vs 0  $\mu\text{mol/L}$  SB203580 group.

protein interactions<sup>[42]</sup>. Phosphorylation of one inhibitory site targeted by multiple kinases determines Cdc25 activation. During interphase, Cdc25 activity is suppressed by both phosphorylation and subsequent binding with a small acidic protein<sup>[43]</sup>. As a result, Cdc2/Cyclin B1 complexes remain phosphorylated and inactive, and thus the cells become arrested at the G<sub>2</sub>/M phase. In our study, we found that telekin effectively inhibited cell proliferation and induced apoptosis and G<sub>2</sub>/M phase arrest.

In conclusion, treating cells with telekin induces ROS generation and increases the level of phospho-p38, phospho-MAPKAPK-2, phospho-Cdc25A, and phospho-Cdc2; furthermore, telekin decreases the level of Cdc25A, Cdc2, and Cyclin B1. These results suggest that the p38 pathway may be involved in the cell cycle arrest at the G<sub>2</sub>/M phase induced by telekin. Our findings in the present study provide a mechanism for the cytotoxic properties of telekin in hepatocellular carcinoma cells.

### Acknowledgements

This work was supported by grants from the National Natural Science Foundation of China (No 81273532).

### Author contribution

Prof Xia LI designed the research and revised the manuscript; Lin LI and Bei-bei ZHENG conducted the research, analyzed the data, and wrote the paper; Li-sha MA, Xiao SUN, Juan-juan CHANG, and Wei-dong XIE helped with portions of the research.

### References

- Zheng SE, Xiong S, Lin F, Qiao GL, Feng T, Shen Z, et al. Pirarubicin inhibits multidrug-resistant osteosarcoma cell proliferation through induction of G<sub>2</sub>/M phase cell cycle arrest. *Acta Pharmacol Sin* 2012; 33: 832–8.
- Wang HC, Chung PJ, Wu CH, Lan KP, Yang MY, Wang CJ, et al. Polyphenolic extract inhibits hepatocarcinoma cell growth by inducing G<sub>2</sub>/M phase arrest and apoptosis. *J Sci Food Agric* 2011; 91: 178–85.
- Choi YH, Lee WH, Park KY, Zhang L. p53-independent induction of p21 (WAF1/CIP1), reduction of cyclin B1 and G<sub>2</sub>/M arrest by the isoflavone genistein in human prostate carcinoma cells. *Jpn J Cancer Res* 2000; 91: 164–73.
- Hartwell LH, Kastan MB. Cell cycle control and cancer. *Science* 1994; 266: 1821–8.
- Khaled AR, Bulavin DV, Kittipatarin C, Li WQ, Alvarez M, Kim K, et al. Cytokine-driven cell cycling is mediated through Cdc25A. *J Cell Biol* 2005; 169: 755–63.
- Shen T, Huang S. The role of Cdc25A in the regulation of cell proliferation and apoptosis. *Anticancer Agents Med Chem* 2012; 12: 631–9.
- Karlsson-Rosenthal C, Millar JB. Cdc25: mechanisms of checkpoint inhibition and recovery. *Trends Cell Biol* 2006; 16: 285–92.
- Boutros R, Dozier C, Ducommun B. The when and wheres of CDC25 phosphatases. *Curr Opin Cell Biol* 2006; 18: 185–91.
- Takenaka K, Moriguchi T, Nishida E. Activation of the protein kinase p38 in the spindle assembly checkpoint and mitotic arrest. *Science* 1998; 280: 599–602.
- Johnson GL, Lapadat R. Mitogen-activated protein kinase pathways mediated by ERK, JNK, and p38 protein kinases. *Science* 2002; 298: 1911–2.
- Jin S, Tong T, Fan W, Fan F, Antinore MJ, Zhu X, et al. GADD45-induced cell cycle G<sub>2</sub>-M arrest associates with altered subcellular distribution of cyclin B1 and is independent of p38 kinase activity. *Oncogene* 2002; 21: 8696–704.
- Martin-Blanco E. p38 MAPK signalling cascades: ancient roles and new functions. *Bioessays* 2000; 22: 637–45.
- Bulavin DV, Higashimoto Y, Popoff IJ, Gaarde WA, Basrur V, Potapova O, et al. Initiation of a G<sub>2</sub>/M checkpoint after ultraviolet radiation requires p38 kinase. *Nature* 2001; 411: 102–7.
- Ding XL, Husseman J, Tomashevski A, Nochlin D, Jin LW, Vincent I. The cell cycle Cdc25A tyrosine phosphatase is activated in degenerating postmitotic neurons in Alzheimer's disease. *Am J Pathol* 2000; 157: 1983–90.
- Goloudina A, Yamaguchi H, Chervyakova DB, Appella E, Fornace AJ Jr, Bulavin DV. Regulation of human Cdc25A stability by Serine 75 phosphorylation is not sufficient to activate a S phase checkpoint. *Cell Cycle* 2003; 2: 473–8.
- Efferth T. Cancer therapy with natural products and medicinal plants. *Planta Med* 2010; 76: 1035–6.
- Paukku Y, Rasulev B, Syrov V, Khushbaktova Z, Leszczynski J. Structure-hepatoprotective activity relationship study of sesquiterpene lactones: A QSAR analysis. *Int J Quantum Chem* 2009; 109: 17–27.
- Li XW, Weng L, Gao X, Zhao Y, Pang F, Liu JH, et al. Antiproliferative and apoptotic sesquiterpene lactones from *Carpesium faberi*. *Bioorg Med Chem Lett* 2011; 21: 366–72.
- Lee J, Min B, Lee S, Na M, Kwon B, Lee C, et al. Cytotoxic sesquiterpene lactones from *Carpesium abrotanoides*. *Planta Med* 2002; 68: 745–7.
- Zheng B, Wu L, Ma L, Liu S, Li L, Xie W, et al. Telekin induces apoptosis associated with the mitochondria-mediated pathway in human hepatocellular carcinoma cells. *Biol Pharm Bull* 2013; 36: 1118–25.
- Xie WD, Wang XR, Ma LS, Li X, Row KH. Sesquiterpenoids from *Carpesium divaricatum* and their cytotoxic activity. *Fitoterapia* 2012; 83: 1351–5.
- Kumar S, Jiang MS, Adams JL, Lee JC. Pyridinylimidazole compound SB 203580 inhibits the activity but not the activation of p38 mitogen-activated protein kinase. *Biochem Biophys Res Commun* 1999; 263: 825–31.
- Clerk A, Sugden PH. The p38-MAPK inhibitor, SB203580, inhibits cardiac stress-activated protein kinases/c-Jun N-terminal kinases (SAPKs/JNKs). *FEBS Lett* 1998; 426: 93–6.
- Shi X, Zhou B. The role of Nrf2 and MAPK pathways in PFOS-induced oxidative stress in zebrafish embryos. *Toxicol Sci* 2010; 115: 391–400.
- Zafarullah M, Li WQ, Sylvester J, Ahmad M. Molecular mechanisms of N-acetylcysteine actions. *Cell Mol Life Sci* 2003; 60: 6–20.
- Hamada S, Fujita S. DAPI staining improved for quantitative cytofluorometry. *Histochemistry* 1983; 79: 219–26.
- Coleman AW, Maguire MJ, Coleman JR. Mithramycin- and 4'-6-diamidino-2-phenylindole (DAPI)-DNA staining for fluorescence microspectrophotometric measurement of DNA in nuclei, plastids, and virus particles. *J Histochem Cytochem* 1981; 29: 959–68.
- Innocente SA, Abrahamson JL, Cogswell JP, Lee JM. p53 regulates a G<sub>2</sub> checkpoint through cyclin B1. *Proc Natl Acad Sci U S A* 1999; 96: 2147–52.
- Liu SS, Wang YF, Ma LS, Zheng BB, Li L, Xie WD, et al. 1-Oxoeudesm-11(13)-eno-12,8a-lactone induces G<sub>2</sub>/M arrest and apoptosis of

- human glioblastoma cells *in vitro*. *Acta Pharmacol Sin* 2013; 34: 271–81.
- 30 Lin CC, Lin SY, Chung JG, Lin JP, Chen GW, Kao ST. Down-regulation of cyclin B1 and up-regulation of Wee1 by berberine promotes entry of leukemia cells into the G<sub>2</sub>/M-phase of the cell cycle. *Anticancer Res* 2006; 26: 1097–104.
- 31 Qanungo S, Wang M, Nieminen AL. *N*-acetyl-L-cysteine enhances apoptosis through inhibition of nuclear factor-kappaB in hypoxic murine embryonic fibroblasts. *J Biol Chem* 2004; 279: 50455–64.
- 32 Liao QC, Xiao ZS, Qin YF, Zhou HH. Genistein stimulates osteoblastic differentiation via p38 MAPK-Cbfa1 pathway in bone marrow culture. *Acta Pharmacol Sin* 2007; 28: 1597–602.
- 33 Chen JT, Fong YC, Li TM, Liu JF, Hsu CW, Chang CS, *et al*. DDTD, an isoflavone derivative, induces cell apoptosis through the reactive oxygen species/apoptosis signal-regulating kinase 1 pathway in human osteosarcoma cells. *Eur J Pharmacol* 2008; 597: 19–26.
- 34 Kumar S, McDonnell PC, Gum RJ, Hand AT, Lee JC, Young PR. Novel homologues of CSBP/p38 MAP kinase: activation, substrate specificity and sensitivity to inhibition by pyridinyl imidazoles. *Biochem Biophys Res Commun* 1997; 235: 533–8.
- 35 Lee JC, Kassis S, Kumar S, Badger A, Adams JL. p38 mitogen-activated protein kinase inhibitors – mechanisms and therapeutic potentials. *Pharmacol Ther* 1999; 82: 389–97.
- 36 Kulisz A, Chen N, Chandel NS, Shao Z, Schumacker PT. Mitochondrial ROS initiate phosphorylation of p38 MAP kinase during hypoxia in cardiomyocytes. *Am J Physiol Lung Cell Mol Physiol* 2002; 282: L1324–9.
- 37 Wuyts WA, Vanaudenaerde BM, Dupont LJ, Demedts MG, Verleden GM. *N*-acetylcysteine reduces chemokine release via inhibition of p38 MAPK in human airway smooth muscle cells. *Eur Respir J* 2003; 22: 43–9.
- 38 Olson JM, Hallahan AR. p38 MAP kinase: a convergence point in cancer therapy. *Trends Mol Med* 2004; 10: 125–9.
- 39 Hsu YL, Kuo PL, Lin LT, Lin CC. Asiatic acid, a triterpene, induces apoptosis and cell cycle arrest through activation of extracellular signal-regulated kinase and p38 mitogen-activated protein kinase pathways in human breast cancer cells. *J Pharmacol Exp Ther* 2005; 313: 333–44.
- 40 Jin Y, Fan Y, Yan EZ, Liu Z, Zong ZH, Qi ZM. Effects of sodium ferulate on amyloid-beta-induced MKK3/MKK6-p38 MAPK-Hsp27 signal pathway and apoptosis in rat hippocampus. *Acta Pharmacol Sin* 2006; 27: 1309–16.
- 41 Rane MJ, Coxon PY, Powell DW, Webster R, Klein JB, Pierce W, *et al*. p38 Kinase-dependent MAPKAPK-2 activation functions as 3-phosphoinositide-dependent kinase-2 for Akt in human neutrophils. *J Biol Chem* 2001; 276: 3517–23.
- 42 Hutchins JR, Clarke PR. Many fingers on the mitotic trigger: post-translational regulation of the Cdc25C phosphatase. *Cell Cycle* 2004; 3: 41–5.
- 43 Margolis SS, Perry JA, Weitzel DH, Freel CD, Yoshida M, Haystead TA, *et al*. A role for PP1 in the Cdc2/Cyclin B-mediated positive feedback activation of Cdc25. *Mol Biol Cell* 2006; 17: 1779–89.